MECHANICAL PROPERTIES OF RE-EXTRUDED $SrFe_{12}O_{19}$(OP-71)/PA12 FILAMENTS VIA TWIN-SCREW EXTRUSION FOR FUSED FILAMENT FABRICATION

Camila Belduque[1], Tanjina Ahmed[2], Wilhelmus Geerts[2,3], Subash Panta[1], Harrison Thramann[1], Liam Omer[1], and Jitendra Tate[1,2,*]

Texas State University
601 University Drive, San Marcos, TX,78666
[1]Ingram School of Engineering
[2]Materials Science Engineering and Commercialization Program
[3]Department of Physics
[*]JT31@Txstate.edu; 512-245-1826

ABSTRACT

The most employed permanent and soft magnetic materials, such as Strontium Ferrite ($SrFe_{12}O_{19}$) is attractive to be dispersed in polymers such as polyamides or ABS to obtain new composites in the additive manufacturing industry. Specifically fused filament fabrication offers a low cost, accessible, and environmentally friendly process. Products such as MRI devices, robots for drug delivery and automotive parts are some of the potential applications that can be developed given a highly filled matrix with homogeneously dispersed magnetic fillers. Twin-screw extrusion is recognized as one of the efficient methods to obtain uniform dispersion of magnetic fillers. Uniform dispersion is key factor in enhancement in mechanical and magnetic properties. In this project, 50wt% $SrFe_{12}O_{19}$/Pa12 magnetic powder was dispersed in PA12 matrix using twin-screw extrusion. Mechanical properties are analyzed in both extruded and re-extruded composites using MTS 810 following ASTM standards. Double pass extruded $SrFe_{12}O_{19}$/Pa12 (OP-71/PA12D) samples exhibited unprecedented tensile and flexural strength increases compared to both neat PA12 and single pass extruded $SrFe_{12}O_{19}$/Pa12 (OP-71/PA12).

Keywords: Additive manufacturing, Polymer-matrix composites (PMCs), magnetic properties, Twin-screw extrusion, Tensile Mechanical Testing, Flexural Mechanical Testing.

Corresponding author: Jitendra Tate, JT31@txstate.edu; 512-245-1826.

DOI: (will be filled by SAMPE)

1. INTRODUCTION

Polymer composites offer extensive benefits in production flexibility and material properties in comparison to traditional materials such as metals and neat polymers. From high specific strength to low-cost production methods, composites offer both industrial and academic opportunities for innovation. One of the key innovative production methods being explored for polymer composites is additive manufacturing. Although Fused Filament Fabricated (FFF) magnetic polymer composites exhibit lower maximum magnetic potential and operational temperatures compared with sintered magnets, the production flexibility offered by additive manufacturing enables composites with unique magnetic properties. In addition, the polymeric properties inherited by the composite such as electrical resistivity and mechanical property improvements provide motivation for further explorations of magnetic composites. Medical and industrial applications relating to robotic locomotion, electromagnetic shielding, and composite Halbach arrays have already shown promising results [10,11,12]. The use of Magnetic Field Assisted Additive Manufacturing (MFAAM) enables designers to tune magnetic material properties of products with variable isotropy and homogeneity. Currently, MFAAM devices are the only production method to produce such magnetic materials.

Ferrite powders have entered academic research as a potential magnetic filler within polymer composites. Ferrites are resistant to oxidation and corrosion extending the viable period of usability. In addition, they are lower cost the other rare earth magnet materials. Strontium Ferrites ($SrFe_{12}O_{19}$) are easily sourced in small particle sizes that possess single domains. The single domain alignment of evenly disperse particles allow for magnetic polymer composites to be produced with a preferred field orientation [2,3]. These fillers exhibit low magnetic moment density in comparison to Iron and Rare Earth Magnetics while maintaining a hysteresis between soft magnets and hard magnets. $SrFe_{12}O_{19}$ typical value of remanence is 0.36 T, coercivity of 320 kA/m, and maximum energy product of 25000 T.

Previous research has investigated both the magnetic and mechanical performance of ferrite polymer composites. Hanemann et al, observed the mechanical properties of Barium Ferrites within Acrylonitrile Butadiene Styrene (ABS) polymer matrix and observed a reduction in ultimate tensile stress and strain within the composite as ferrite loading was increased [6]. Huber et al. found similar degradation of tensile properties in $SrFe_{12}O_{19}$ within Polyamide-12 (PA-12) composites [9]. As Strontium Ferrite filler content increased, ultimate tensile stress decreased. However, the $SrFe_{12}O_{19}$/PA-12 composite exhibited a significant increase in ultimate tensile strain. In addition, additively manufacturing $SrFe_{12}O_{19}$/PA-12 composite printed in presence of an external field exhibited 40% higher remanence than that of samples printed without external fields. Employing the anisotropic properties of ferrite composites, Kallaste et al. exhibited the potential of $SrFe_{12}O_{19}$ composites to create Halbach arrays for power generation. The resulting composite exhibited an oriented magnetic field that allowed for a reduction in weight in comparison to the required magnet using pure strontium ferrite with isotropic properties [12].

Characterization of hard magnetic materials produced using additive manufacturing is limited. Commercially, only one magnetic filament for FFF additive manufacturing is available from Protopasta using a soft magnetic iron filler within polylactic acid (PLA) polymer matrix. Studies have shown these materials to be brittle, inhibiting the potential uses within functional magnetic or structural applications [14]. PA-12 exhibits higher toughness and overall mechanical benefits

in comparison to PLA. This study targets the manufacturing of $SrFe_{12}O_{19}$/PA-12 filament composite (OP-71/PA12) for using in FFF additive manufacturing. The FFF process was adapted to print anisotropic magnets by applying an external field during printing. Previous studies have noted the effects of voiding, filler dispersion, and poor interfacial reactivity between composite materials can contribute to the degradation of mechanical properties in composite systems [7]. Therefore, this paper aims to discuss the effect of repalletization and extrusion of OP-71 filament within a twin-screw extruder to reduce void content and increase filler dispersion within the PA-12 matrix. The dual extruded OP-71 filament (OP-71/PA12D) was mechanical and thermally compared to OP-71/PA12 and neat PA12.

2. Experimentation

To improve the dispersion of the fillers in the PA12, both components are mixed in a Thinky ARV-310 Planetary Centrifugal Mixer. A 50wt% filler concentration of each composite is loaded at 500 rpm, five cycles of three minutes of mixing and three minutes of resting in ambient pressure. Twenty ceramic balls of 10 mm diameter were added to the containers. Figure 1 illustrated material changes throughout mixing durations.

Figure 1. Fillers and PA12 at zero, two and five mixing cycles of three minutes.

The extrusion process is conducted in a Process 11 Twin Screw Extruder. It has nine temperature zones to gradually melt, mix, and extrude the materials. Vacuum is applied at stage seven. For all composites, these values were set as follows: z_1: cool zone, z_2: 220°C, z_3: 230°C, z_4: 230°C, z_5: 240°C, z_6:240°C, z_7:240°C, z_8:230°C, die: 220°C. This temperature range allowed the composite material to flow continuously. Neat PA12 was extruded with a lower temperature range (highest zone temperature at 220°C) to avoid thermal degradation. The same path was attempted to produce the composites. However, the viscosity of the new material was too high and increased the torque in the extruder beyond the allowed limit. Consequently, the temperature was increased to avoid damaging the machine and obtain a continuous filament. Figure 2 shows the Process 11 Twin Screw Extruder used and the RPM set at the feeder and screws for each composite.

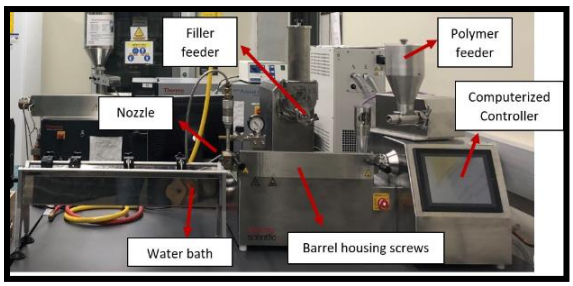

Material	Feeder RPM	Screws RPM	Filament Diameter [mm]
PA12	55	120	1.55 ± 0.03
OP-71/PA12	50	170	1.3 ± 0.03

Figure 2. Process 11 Twin-Screw Extruder and table showing parameters used to create each composite filament and final diameters.

Twin screw extruders have previously been characterized with inconsistent filament diameter. This is commonly solved by pelletizing the material and extruding or upgrading the machine with a melt pump [16]. After extrusion of the OP-71/PA12 filament, the material was repelletized using a Kingston KMT 5V Manual Mill and extruded for a second time using the Process 11 Twin Screw Extruder to produce a double passed filament, OP-71/PA12D.

2.1 Fused Filament Fabrication

A CraftBot XL3 was used to print the type I samples required by the ASTM D638 for tension testing. The first printed sample had a thickness 0.4 mm larger than the designed one. Therefore, the thickness was adjusted in the CAD file to compensate for such increment. Flexure properties were done following the ASTM D790, a 7 mm x 12.7 mm x 3.25 mm rectangle was designed. The 3D printing was performed using a 0.4 mm hardened steel nozzle and layer size of 0.2 mm. A temperature of 235°C was intended for FFF production to decrease thermal stresses on the materials but it triggered obstructions several times. Therefore, this parameter was gradually increased up to 270°C, the optimum value at which all the composites could be printed with no difficulties. Additionally, metallic and glass beds heated at 95°C were used to deposit the specimens. Due to bed adhesion difficulties, the fans were turned off and glue and paper were needed to guarantee adhesion of the first two layers to the bed, which were printed at 50% speed.

2.2 Mechanical and Thermal Characterization

Thermogravimetric Analysis (TGA) and Differential Scanning Calorimetry (DSC) were performed on a TA Instruments SDT650. Flexure and tension behavior of 3D printed samples is determined according to ASTM D790 and D638 using an MTS Servo hydraulic 810 mechanical testing machine.

3. RESULTS

3.1 Density Measurements

Table 2. Density measurements of composites and neat PA12 according to ASTM 792.

Density (g/cm3)		
PA12	OP-71/PA12 Single Extrusion	OP-71/PA12 Secondary Extrusion
1.04	1.40	1.60

The density of both the composites and neat PA12 were obtained conforming to ASTM D792. Samples were manufacturing per the ASTM standard requirement to create two samples of each material with a volume higher than 1 cm^3 and soft edges. Density changes between single pass extrusion and secondary pass extrusion seem attributable to potential reductions in void and filament porosity.

3.2 Thermogravimetric Analysis and Differential Scanning Calorimetry

A TA Instruments SDT 650 is used to perform TGA and DSC analyses on the composites and neat PA-12. All tests were performed with a heating rate of 20°C/min up to 600°C in a nitrogen environment. Figure 7 displays the TGA and Derivate TGA overlay on neat PA12, and the composites created. Figure 8 Exhibits the differential calorimetry scanning of each composite in comparison to neat PA-12. The neat PA-12 loses weight starting at 350°C and ends decomposition at 500°C resulting in a 2% residual mass that remains up until 600°C. In contrast, the composites start degrading at around 410°C. Strontium ferrite has been reported to have thermal anisotropy, it transfers the heat through the in-plane direction more efficiently than through the cross section direction [19]. Peak degradation occurred at 455°C for neat PA-12 compared to both OP-71/PA12 and OP-71/PA12D peak degradation at 480°C. Differential Scanning Calorimetry noted a significant change in heat flow of double pass extruded OP-71/PA12D at 180°C and 465°C. Anisotropic thermal properties of strontium ferrite in tandem with in-plane particle orientation as a result of a second extrusion pass caused a significant endothermic peak at 465°C. Orientation of ferrite crystals in parallel with the filament caused inhibition of heat flow until polymer degradation in which orientation of the ferrite particles were no longer constrained. The unconstrained ferrite filler was then heated at a high rate through its in-plane direction. This large peak was not seen in the single pass extruded composite due to randomly oriented filler.

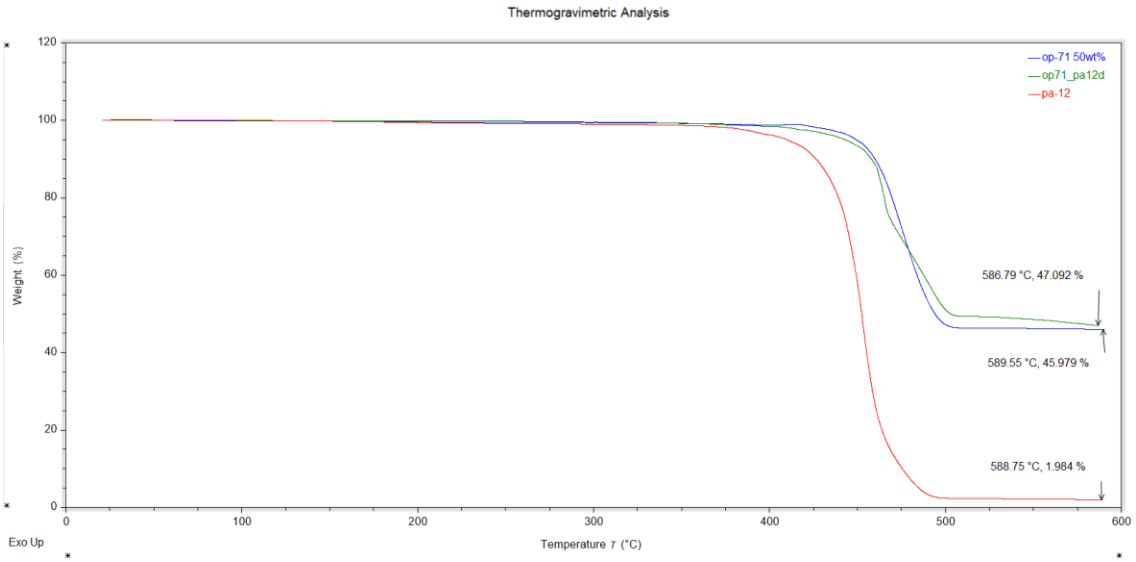

Figure 7. TGA results on neat PA12 and composites with a 50wt% loading level.

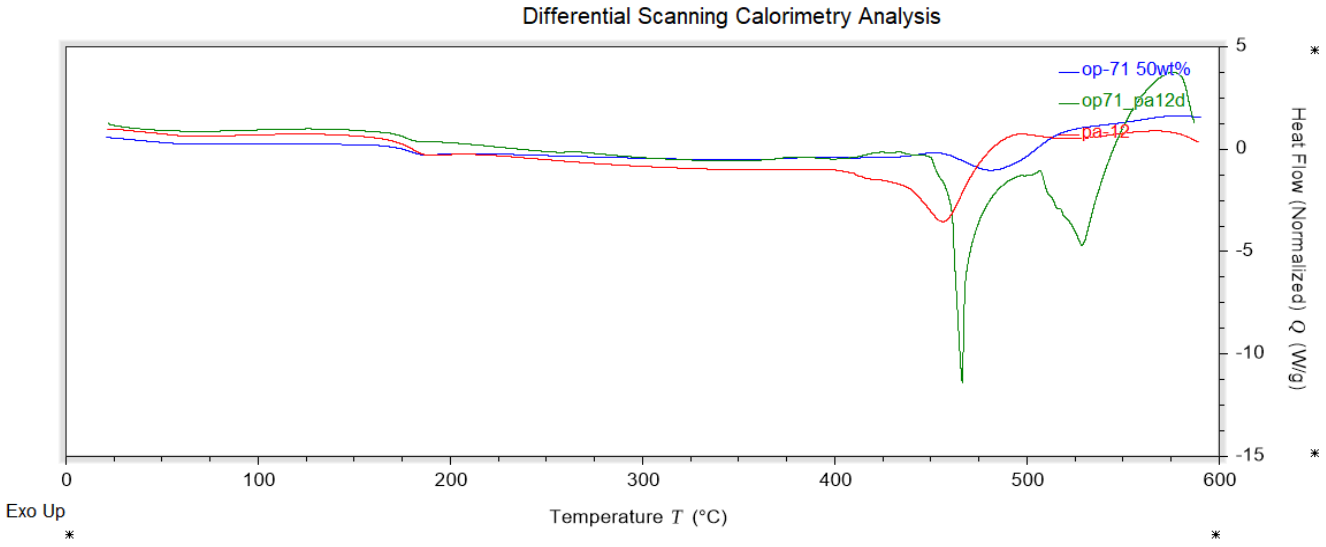

Figure 8. Heat Cycle heat flow results on neat PA-12 and composites with a 50wt% loading level.

3.3 Mechanical Properties

Samples of each composite and neat PA12 were tested under flexure and tension in a Servohydraulic Material Testing System 810 following ASTM D790 and ASTM D638, respectively. There is a minimal decrease in the flexural strength of PA-12 when loaded with 50wt% of $SrFe_{12}O_{19}$ after a single pass extrusion production method. However, double pass extrusion PA12 when loaded with 50wt% of $SrFe_{12}O_{19}$ exhibited a significant increase in both flexural modulus and strength by 200% and 103%, respectively in comparison to neat PA12. In previous studies, at 40wt% of $SrFe_{12}O_{19}$/PA12 these properties increased by 18% and 30% respectively. The significant change in flexural strength of double passed extrusion OP-71/PA12D is potentially attributable to a work hardening and homogenizing effect of multiple extrusion passes. In addition, the second pass may have ensured low porosity leading to high quality layer adhesion during sample production using FFF additive manufacturing.

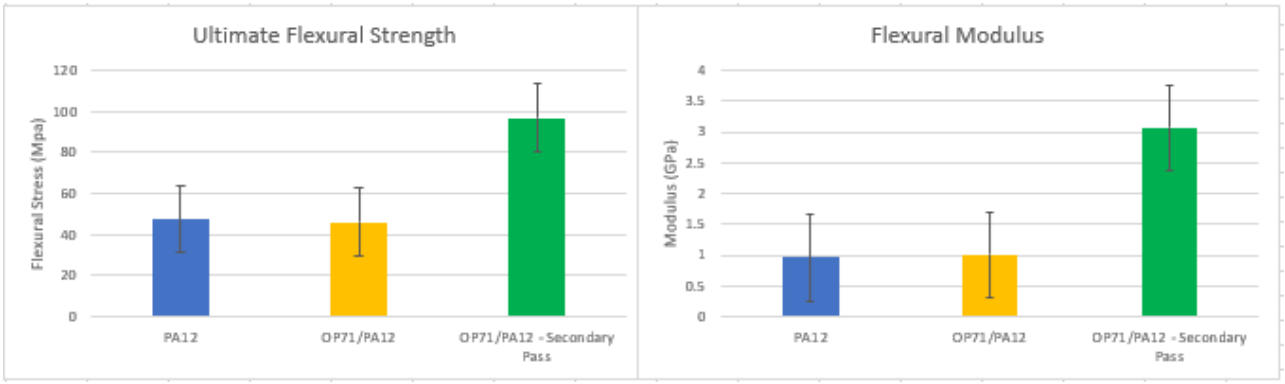

Figure 9. Flexural modulus and flexural strength values obtained from the composites manufactured at 50wt% loading levels.

The ultimate tensile strength of OP-71/PA12D compared to neat PA12 and OP-71/PA12 increased by 74.8%. Tensile modulus had no significant change between neat PA-12, OP-71/PA12, and OP-71/PA12D. Increase in tensile strength may be attributable to a significantly more homogenous dispersion of magnetic filament particles resulting in a reduction of stress concentrations at aggregates. In addition, the secondary extrusion of filament may have reduced porosity in the filament improving printing quality for tensile samples.

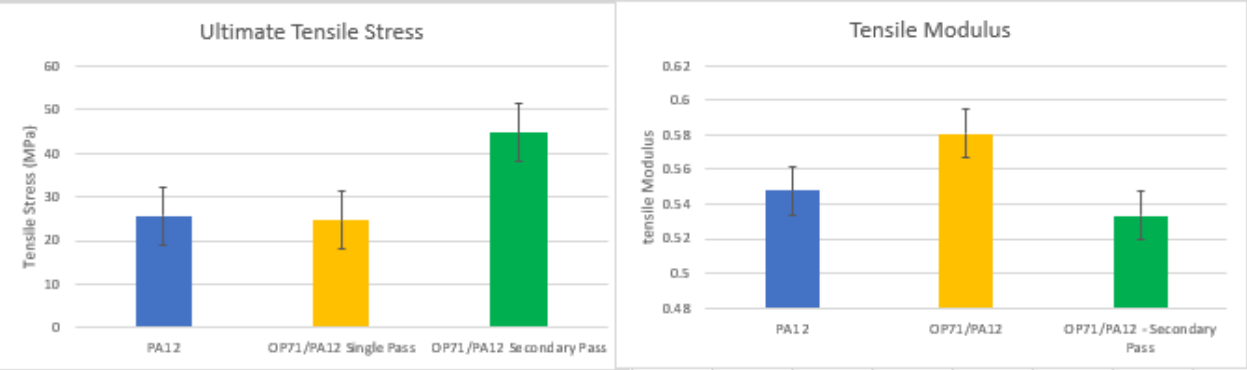

Figure 11. Ultimate Tensile strength and tensile modulus of polymer composite samples compared to neat polyamide-12.

4 CONCLUSIONS

Magnetic filament composites of PA12 filled with 50wt% $SrFe_{12}O_{19}$ magnetic powder were successfully manufactured using multiple passes of twin screw extrusion. The temperature range required to produce these composites is higher than that of the control material due to the rheological changes exhibited within the composite material.

TGA and DSC analyses performed on all the materials show an improved heat flow in the composites compared to that of the neat PA12. Additionally, all the composites show an increase in remainder weight % (compared to addition of 50wt% magnetic powder).

Two nozzle sizes were used during 3D printing to analyze the magnetic behavior of the materials. The effects of 55 kOe magnetic field on heating section of 3D printer has potentially caused magnetic particles clogging inside the nozzle and resulting in excess PA12 in the printed samples, changing the filler concentration, and leading to a decrease in magnetic properties.

The tensile modulus of the OP-71/PA12 composite increased by 25.13% while OP-71/PA12D showed no significant change compared to neat PA12. The ultimate tensile strength of OP-71/PA12D compared to neat PA12 and OP-71/PA12 increased by 74.8%. The flexural strength is improved by 100% in OP-71/PA12D composites. Additionally, the flexural modulus increased by 7.5% and 200% for OP-71/PA12 and OP-71/PA12D, respectively. The use of multiple extrusion passes shows obvious benefits in terms of tensile and flexural strength. Further investigation is required to determine the changes in magnetic performance of filaments produced using multi pass extrusion.

5. REFERENCES

1. Huber, Mitteramskogler, Goertler, Teliban, Groenefeld and Suess. Additive Manufactured Polymer-Bonded Isotropic NdFeB Magnets by Stereolithography and Their Comparison to Fused Filament Fabricated and Selective Laser Sintered Magnets. Materials (Basel, Switzerland). 2020. 10.3390/ma13081916

2. Lagorce and Allen. Magnetic and mechanical properties of micromachined strontium ferrite/polyimide composites. Journal of Microelectromechanical Systems. 1997. 10.1109/84.650127

3. Ketov, Yagodkin and Menushenkov. Structure and magnetic properties of strontium ferrite anisotropic powder with nanocrystalline structure. Journal of Alloys and Compounds. 2011. https://doi.org/10.1016/j.jallcom.2010.09.184

4. B. D. Cullity and Graham, Magnetic Anisotropy. Journal. 2008.

5. Granados-Miralles, Saura-Múzquiz, Bøjesen, Jensen, Andersen and Christensen. Unraveling structural and magnetic information during growth of nanocrystalline SrFe12O19. Journal of Materials Chemistry C. 2016. 10.1039/C6TC03803D

6. Hanemann, Syperek and Nötzel. 3D Printing of ABS Barium Ferrite Composites. Materials (1996-1944). 2020. 10.3390/ma13061481

7. Kallagunta and Tate. Low-velocity impact behavior of glass fiber epoxy composites modified with nanoceramic particles. Journal of Composite Materials. 2019. 10.1177/0021998319893435

8. Shrivastava, Shrivastava, 5 - Plastics Processing. William Andrew Publishing, Journal. 2018.

9. Huber, Cano, Teliban, Schuschnigg, Groenefeld and Suess. Polymer-bonded anisotropic SrFe12O19 filaments for fused filament fabrication. Journal of Applied Physics. 2020. 10.1063/1.5139493

10. Hu, Lum, Mastrangeli and Sitti. Small-scale soft-bodied robot with multimodal locomotion. Nature. 2018. 10.1038/nature25443

11. Iqbal, Khatoon, Kotnala and Ahmad. Mesoporous strontium ferrite/polythiophene composite: Influence of enwrappment on structural, thermal, and electromagnetic interference shielding. Composites Part B: Engineering. 2019. https://doi.org/10.1016/j.compositesb.2019.107143

12. Kallaste, Kilk, Belahcen, Vaimann and Janson, Demagnetization in Permanent Magnet Slotless Generator Using Halbach Array. Journal. 2012.

13. Bollig, Patton, Mowry and Nelson-Cheeseman. Effects of 3D Printed Structural Characteristics on Magnetic Properties. IEEE Transactions on Magnetics. 2017.

10.1109/TMAG.2017.2698034

14. Bollig, Hilpisch, Mowry and Nelson-Cheeseman. 3D printed magnetic polymer composite transformers. Journal of Magnetism and Magnetic Materials. 2017. https://doi.org/10.1016/j.jmmm.2017.06.070

15. Zakaria, Abd, Abd, Haroun, Elfaki and Elgani, Explanation of the Effect of Magnetic Field on laser Intensity on the Basic of Generalized Special Relativity. Journal. 2014.

16. Martin, Repka, Langley and DiNunzio, Twin Screw Extrusion for Pharmaceutical Processes. New York, NY: Springer New York, Journal. 2013.

17. Ponsar, Wiedey and Quodbach. Hot-Melt Extrusion Process Fluctuations and their Impact on Critical Quality Attributes of Filaments and 3D-printed Dosage Forms. Pharmaceutics. 2020. 10.3390/pharmaceutics12060511

18. Mørup, Hansen and Frandsen, Andrews, Scholes and Wiederrecht, 1.14 - Magnetic Nanoparticles. Amsterdam: Academic Press, Journal. 2011.

19. Volodchenkov, Ramirez, Samnakay, Salgado, Kodera, Balandin and Garay. Magnetic and thermal transport properties of SrFe12O19 permanent magnets with anisotropic grain structure. Materials & Design. 2017. https://doi.org/10.1016/j.matdes.2017.03.082

20. González, Parga, Moreno, Ramos, Martínez, Martínez and Vazquez. Synthesis and Characterisation of Strontium Hexaferrite Using an Electrocoagulation by-Product. Journal of Chemical Research. 2016. 10.3184/174751916X14533976548491

21. Pigliaru, Rinaldi, Ciccacci, Norman, Rohr, Ghidini and Nanni. 3D printing of high performance polymer-bonded PEEK-NdFeB magnetic composite materials. Functional Composite Materials. 2020. 10.1186/s42252-020-00006-w